

# Critical gradient turbulence optimization toward a compact stellarator reactor concept

G. T. Roberg-Clark,\* G. G. Plunk, P. Xanthopoulos, C. Nührenberg, S. A. Henneberg, and H. M. Smith

*Max-Planck-Institut für Plasmaphysik, D-17491, Greifswald, Germany*

(Dated: January 18, 2023)

Integrating turbulence into stellarator optimization is shown by targeting the onset for the ion-temperature-gradient mode, highlighting effects of parallel connection length, local magnetic shear, and flux surface expansion. The result is a compact quasi-helically symmetric stellarator configuration, admitting a set of uncomplicated coils, with significantly reduced turbulent heat fluxes compared to a known stellarator. The new configuration combines low values of neoclassical transport, good alpha particle confinement, and Mercier stability at a plasma beta of almost 2%.

*Introduction.*— A primary obstacle for the success of magnetic confinement fusion is the transport caused by instabilities such as the ion temperature gradient (ITG) mode, which is thought to significantly reduce plasma confinement in experiments such as the Wendelstein 7-X stellarator [1–3]. To overcome the losses from such turbulence, a given configuration can be scaled up in size and heating power. A less costly alternative, currently explored, is to shape the magnetic field to alleviate the turbulence. This option could be particularly appealing for reactor scenarios, in which it will likely be difficult to control density profiles via pellet injections [4, 5], since the penetration distance of pellets may be limited in comparison to the minor radius of a reactor.

To achieve turbulence optimization via shaping, several strategies have been developed to reduce the rate that turbulent transport increases (“stiffness”) as a function of the ion temperature gradient [6–10]. Another approach is to target the onset (“critical”) gradient of significant turbulent transport [11–13], which relies primarily on linear physics of ITG modes themselves [14–17] and avoids the hard problem of solving turbulence in the full range of toroidal geometries. Successful optimization has been recently demonstrated using a critical gradient (CG) approach, even leading to reduced stiffness of ITG turbulence in the nonlinear regime [12, 18], but at the apparent cost of MHD stability via the loss of a vacuum magnetic well.

In this Letter, we show that CG optimization can be achieved without compromising MHD stability, or other key properties needed by a stellarator design. Here we target the critical gradient of only the toroidal branch of the ITG mode, based on the assumption that turbulence intensity will be small below this threshold. Our model highlights the familiar stabilizing effects of local shear, but gives greater emphasis to short connection lengths between regions of ‘good’ and ‘bad’ magnetic curvature. The resulting objective function is used via optimization to produce a quasi-helically symmetric (QH) configuration with strongly reduced ITG turbulence, with acceptable levels of neoclassical confinement, alpha particle confinement, coil complexity, and MHD stability,

completing the picture for an initial stellarator concept with improved ion confinement.

*Definitions.*— Following [19], we use the standard gyrokinetic system of equations [20] to describe electrostatic fluctuations destabilized along a thin flux tube tracing a magnetic field line. The ballooning transform [21, 22] is used to separate out the fast perpendicular (to the magnetic field) scale from the slow parallel scale. The magnetic field representation in field following (Clebsch) representation reads,  $\mathbf{B} = \nabla\psi \times \nabla\alpha$ , where  $\psi$  is a flux surface label and  $\alpha$  labels the magnetic field line on the surface. The perpendicular wave vector is then expressed as  $\mathbf{k}_\perp = k_\alpha \nabla\alpha + k_\psi \nabla\psi$ , where  $k_\alpha$  and  $k_\psi$  are constants, so the variation of  $\mathbf{k}_\perp(l)$  stems from that of the geometric quantities  $\nabla\alpha$  and  $\nabla\psi$ , with  $l$  the field-line-following (arc length) coordinate.

We assume Boltzmann-distributed (adiabatic) electrons, thus solving for the perturbed ion distribution  $g_i(v_\parallel, v_\perp, l, t)$ , defined to be the non-adiabatic part of  $\delta f_i$  ( $\delta f_i = f_i - f_{i0}$ ) with  $f_i$  the ion distribution function and  $f_{i0}$  a Maxwellian. The electrostatic potential is  $\phi(\mathbf{l})$ , and  $v_\parallel$  and  $v_\perp$  are the particle velocities parallel and perpendicular to the magnetic field, respectively. The gyrokinetic equation reads

$$iv_\parallel \frac{\partial g}{\partial \ell} + (\omega - \tilde{\omega}_d)g = \varphi J_0(\omega - \tilde{\omega}_*)f_0 \quad (1)$$

where  $\omega$  is the mode frequency,  $\omega_*^T = (Tk_\alpha/q)d\ln T/d\psi(v_\parallel^2/v_T^2 - 3/2)$  is the diamagnetic frequency, and  $J_0 = J_0(k_\perp(l)v_\perp/\Omega(l))$  is the Bessel function of zeroth order. The thermal velocity is  $v_T = \sqrt{2T/m}$ , the thermal ion Larmor radius is  $\rho = v_T/(\Omega\sqrt{2})$ ,  $n$  and  $T$  are the background ion density and temperature,  $q$  is the ion charge,  $\varphi = q\phi/T$  is the normalized electrostatic potential,  $\Omega = qB/m$  is the cyclotron frequency, with  $B = |\mathbf{B}|$ . The magnetic drift frequency in the low  $\beta$  approximation becomes  $\omega_d = (1/\Omega)(\mathbf{k}_\perp \cdot \mathbf{b} \times \boldsymbol{\kappa})(v_\parallel^2 + v_\perp^2/2) = \omega_{d0}(v_\parallel^2 + v_\perp^2/2)$ , with  $\boldsymbol{\kappa} = \mathbf{b} \cdot \nabla \mathbf{b}$  and  $\mathbf{b} = \mathbf{B}/B$ . For simplicity in this analysis we set  $k_\psi = 0$ . We rewrite the drift frequency as  $\omega_d(\ell) \propto K_d(\ell) \equiv a^2 \nabla\alpha \cdot \mathbf{b} \times \boldsymbol{\kappa}$ , referring to  $K_d(\ell)$  as the “drift curvature” and to individual regions of bad curvature along the field line (where  $K_d > 0$ ) as “drift wells”. We define a radial coordinate  $r = a\sqrt{\psi/\psi_{edge}}$ , with  $a$  the minor radius corresponding

\* gar@ipp.mpg.de

to the flux surface at the edge, and  $\psi_{edge}$  the toroidal flux at that location. As usual, the temperature gradient scale length is measured relative to the minor radius,  $a/L_T = -(a/T)dT/dr$ . To study the most unstable ITG mode conditions, we neglect certain stabilizing factors such as the density gradient [23, 24] and plasma beta (electromagnetic effects) [25].

Finally, the gyrokinetic system is completed by quasineutrality,

$$\int d^3\mathbf{v} J_{0g} = n(1 + \tau)\varphi, \quad (2)$$

with  $\tau = |q_e|T_i/(q_iT_e)$ ,  $T_e$  the electron temperature, and  $q_e$  the electron charge.

*Toroidal mode threshold.*— It is expected [13, 26, 27] that the onset of toroidal ITG modes, as can be observed in the linear spectrum [17], should lead to noticeable increases in nonlinear heat fluxes. That is to say, the turbulence found below this onset (in the Floquet-like or slab-like regime) is thought to be more benign, transitioning to significant heat losses only for larger gradients (in the toroidal regime).

We therefore focus our attention on the toroidal ITG mode [14, 17, 19, 28] with strongly peaked eigenmode structure that decays within a single drift well. In the standard local (in  $l$ ) theory of toroidal ITG modes [14, 15, 19], the critical gradient is set by the drive parameter  $\kappa_d = R_{\text{eff}}/L_T$ , where  $R_{\text{eff}}$  is the local effective radius of curvature determined by the profile of  $K_d(\ell)$ . This threshold can be computed for general parameter  $b$  by solving the local dispersion relation

$$0 = 2 - \frac{2}{\sqrt{\pi}} \int_0^\infty dx_\perp x_\perp \int_{-\infty}^\infty dx_\parallel \left[ \frac{\omega - \tilde{\omega}_*}{\omega - \tilde{\omega}_d} \right] J_0^2 \exp(-x^2), \quad (3)$$

which upon substitution of  $K_d = a/R_{\text{eff}}$  yields the critical gradient  $R_{\text{eff}}/L_{T,crit} = F(b)$ , where  $F(b)$  can be obtained numerically and is fairly well approximated by

$$\begin{aligned} F(b) &= 2.84 + 4.926 b, b < 0.755 \\ &= 0.0371 + 7.51\sqrt{b}, b \geq 0.755 \end{aligned} \quad (4)$$

In realistic geometry, the threshold is controlled by the extent of drift wells, *i.e.* the parallel connection length  $L_\parallel$ , but this can be related to finite Larmor radius (FLR) stabilization as follows. Note that a toroidal mode must have a drift frequency  $\omega_d \propto k_\alpha$  that exceeds the parallel transit rate  $k_\parallel v_T \sim \pi v_T/L_\parallel$ . Although this can always be satisfied by choice of  $k_\alpha$ , the increase of  $k_\alpha$  comes at the cost of increasing  $b = k_\perp^2 \rho^2$  as  $L_\parallel$  is reduced. Thus, to estimate the critical gradient, we simply determine the minimum value of  $b$  for which the resonance condition is satisfied, *i.e.* that for which  $\omega_d \sim \pi v_T/L_\parallel$ , yielding  $b_{min} = (\pi a |\nabla \alpha| R_{\text{eff}}/L_\parallel)^2$ , and

$$\frac{a}{L_{T,crit}} = \frac{a}{R_{\text{eff}}} F((\pi a |\nabla \alpha| R_{\text{eff}}/L_\parallel)^2) \quad (5)$$

with  $F(b)$  defined as above. The quantities  $R_{\text{eff}}$  and  $L_\parallel$  are in practice computed by identifying and searching the drift wells along a particular field line as presented in [12], while  $a|\nabla \alpha|$  is evaluated at the center of the drift well, effectively approximating it as a constant. In the small- $b$  limit,  $F(b)$  is dominated by the constant term 2.84, close to the value of 2.66 determined or assumed in other works [12, 14, 29], at least for the case  $\tau = 1$ . In the large  $b$  limit, which applies to the flux tubes of both W7-X and HSX, we find, ignoring the small constant  $\simeq 0.04$ , that the formula effectively predicts  $a/L_{T,crit} \sim a^2 |\nabla \alpha| / L_\parallel$ . Perhaps unsurprisingly, then, the threshold for toroidal modes in this regime is dominated by both the gradient of the bi-normal coordinate (linked to expansion of surfaces as well as local magnetic shear [18]) and the parallel connection length, which can be reduced by simply increasing the number of field periods in a configuration. Indeed, an experimental realization of this strategy can already be seen in the 10 field-period LHD heliotron, whose favorable ITG turbulence properties relative to W7-X have been demonstrated [30]. More generally, equation (5) can now be used to rapidly estimate the toroidal ITG threshold on a given magnetic field line.

*Optimization results.*— We use the SIMSOPT software framework [31] to generate a vacuum stellarator configuration with quasi-helical symmetry (QHS) and target a toroidal critical gradient of  $a/L_{T,crit} = 2.90$  at the surface  $r/a = 0.5$ . The stellarator magnetic field is described by a boundary surface given in the Fourier representation  $R(\vartheta, \phi) = \sum_{m,n} R_{m,n} \cos(m\vartheta - 6n\phi)$ ,  $Z(\vartheta, \phi) = \sum_{m,n} Z_{m,n} \sin(m\vartheta - 6n\phi)$ , where we have assumed stellarator symmetry and have set the number of field periods to  $n_{fp} = 6$ . This number was chosen to minimize the parallel connection length without significantly compromising the QH symmetry quality ( $n_{fp} = 4$  cases were also studied). Global zero- $\beta$  equilibria are constructed at each iteration by running the VMEC [32] code, which solves the MHD equations using an energy-minimizing principle, setting the angular resolution to be  $m_{pol} = n_{tor} = 7$ .

Optimization proceeds by treating the above-mentioned Fourier coefficients as parameters and varying them in order to find a least-squares minimization of the specified objective function, which reads

$$f = f_{QS} + f_A + f_{crit} + f_{well} \quad (6)$$

where  $f_A = [\Theta(A - 7.50)]^2$  is the aspect ratio penalty with  $A = R/a$  the aspect ratio output by VMEC,  $\Theta(x)$  is defined to be  $xH(x)$  with  $H(x)$  the Heaviside step function,  $f_{QS}$  is the quasisymmetry residual defined in [33] for QHS with  $n_{fp} = 6$ , and  $f_{crit} = \sum_{\alpha_j} [\Theta(2.90 - a/L_{T,crit}(\alpha_j))]^2$  [eq. (5)] is taken at the surface  $r/a = 0.5$  and summed over the field lines  $\alpha = [0, \pi/8, \pi/4]$ , with each field line extending for 8 poloidal turns, in an attempt to cover the surface. The vacuum magnetic well penalty is  $f_{well} = \sum_{r_k} [\Theta(1 + V''(r_k)/0.001)]^2$  with the surfaces  $(r/a)^2 = [0, 0.1, \dots, 0.90]$  targeted and  $V''(r)$  the second derivative of the flux surface volume with radius.

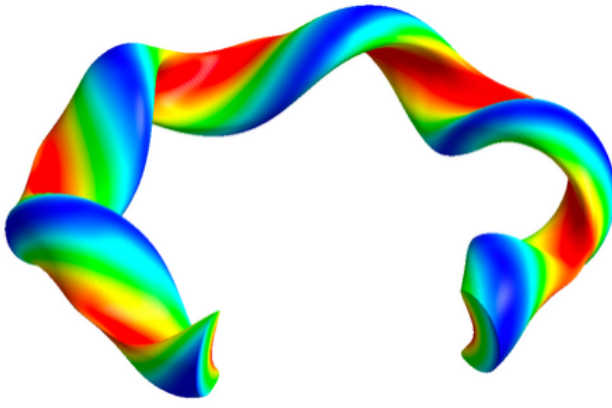


FIG. 1. Boundary surface of QSTK with one field period removed, showing contours of  $B$  in color.

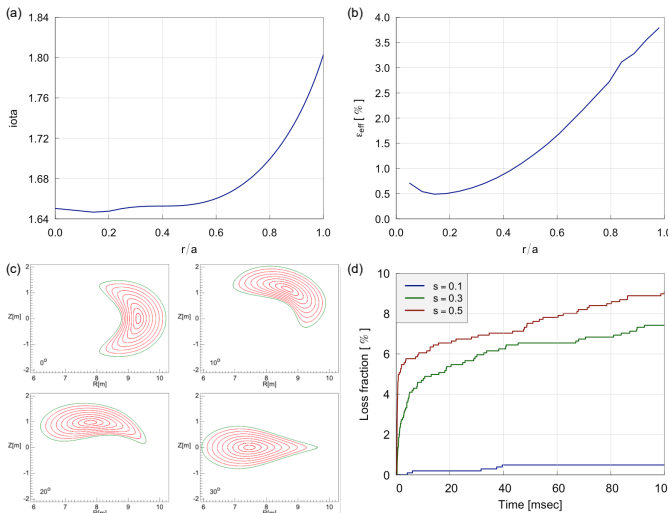


FIG. 2. Properties of QSTK in vacuum. (a) Rotational transform profile. (b) Neoclassical transport coefficient  $\epsilon_{\text{eff}}$  as a function of radius. (c) Toroidal cuts of flux surfaces within one field period. (d) Alpha particle losses for QSTK, rescaled to ARIES-CS minor radius and magnetic field, at various radii [ $s = (r/a)^2$ ].

We calculate the residual  $f_{QS}$  on the surfaces  $(r/a)^2 = [0, 0.1, 0.2, 0.3, 0.4, 0.5]$  as in [18]. The input equilibrium for the optimization was produced by taking a four field period, aspect ratio 6 QH configuration (the “warm start” file from SIMSOPT), optimized for increased  $|\nabla\alpha|$  on the outboard side (see e.g. [18, 34]), and then increasing the number of field periods to 6 in the VMEC input file. The final optimization of the six field period configuration proceeded in two steps, with the boundary Fourier coefficients varied up to  $m_{\text{pol}} = n_{\text{tor}} = (6, 7)$ .

We call the resulting configuration “QSTK” (Quasi-Symmetric Turbulence Konzept), the boundary surface of which is shown in Fig. 1. QSTK has an aspect ratio of 7.5, a volume-averaged magnetic well (0.7%), large rotational transform  $> 1.60$ , a neoclassical transport co-

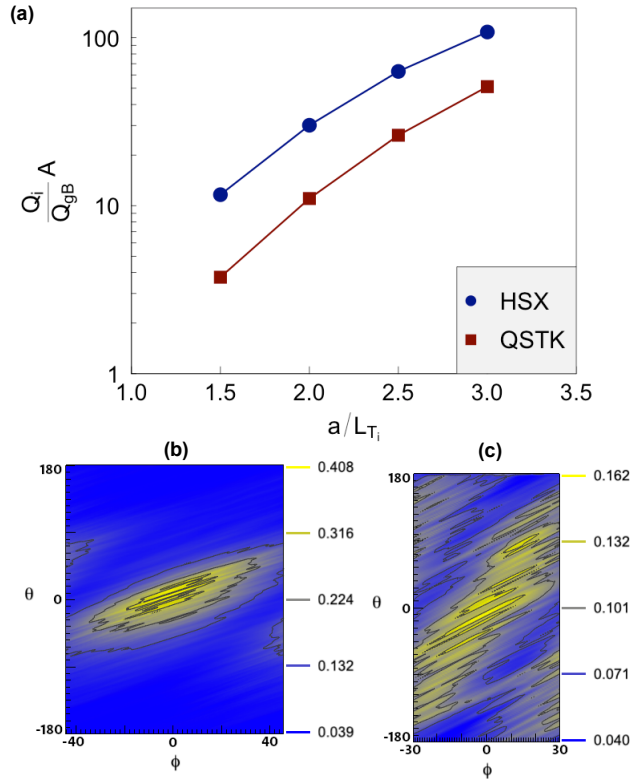


FIG. 3. Full-surface nonlinear gyrokinetic simulations of ITG turbulence comparing HSX to QSTK. (a) Log plot of ion heat flux multiplied by the respective aspect ratio of each configuration. (c) ITG density fluctuations  $\bar{n}/n_0$  in one field period of HSX with  $a/L_{T,crit} = 3$ , plotted in Boozer toroidal ( $\phi$ ) versus poloidal ( $\theta$ ) angles. (d) Same as in (c) but for QSTK.

efficient  $\epsilon_{\text{eff}} < 1\%$  [35] up to roughly half radius, unusually expanded flux surfaces, and low alpha particle losses (< 1%) for particles initialized at  $(r/a)^2 = 0.1$  when rescaled to an ARIES-CS-equivalent [36] minor radius and volume averaged magnetic field strength, using the NEAT code [37, 38] (Fig. 2). Increased neoclassical transport at the edge [reaching  $\epsilon_{\text{eff}} = 4\%$ , Fig. 2(b)] may in fact be beneficial, as it can prevent a particle transport barrier from forming, which might otherwise hinder refueling of plasma in an experimental scenario [39]. All flux tubes evaluated for QSTK, using the model equation (5), are predicted to have  $a/L_{T,crit} \geq 2.90$ .

*ITG turbulence.*— To evaluate the performance of QSTK in vacuum with regard to ITG turbulence we run full-surface nonlinear electrostatic gyrokinetic simulations using the GENE code [40, 41] in comparison with the HSX stellarator experiment [42]. We assume adiabatic electrons, zero density gradient,  $T_e = T_i$ , and simulate fluctuations on the surface  $r/a = 0.5$  for the temperature gradients  $a/L_T = [1.5, 2.0, 2.5, 3.0]$ . In Figs. 3 (a)-(b) we plot the ion heat fluxes in gyro-Bohm units times the aspect ratio of the associated configuration, to adjust for the dependence of energy confinement time on aspect ratio implied by the gyro-Bohm scaling of heat

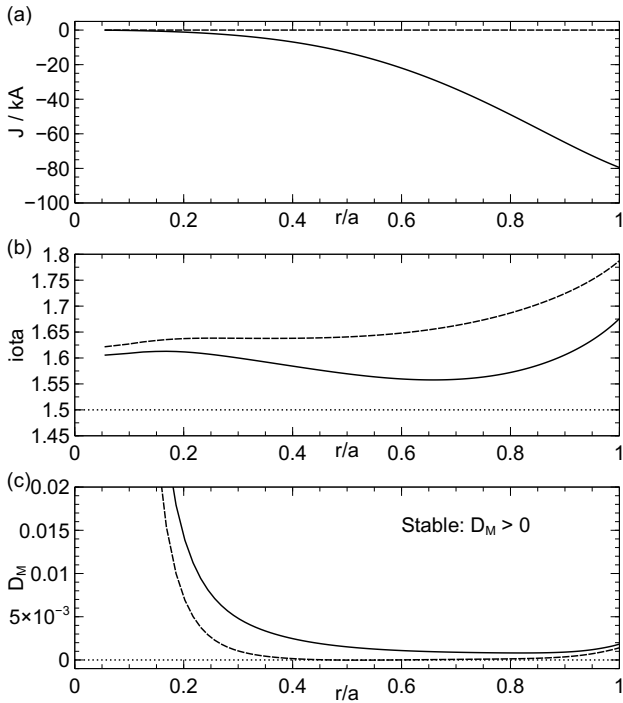


FIG. 4. Bootstrap current and MHD stability of QSTK with an applied pressure profile (see text) at volume-averaged  $\beta = 1.78\%$ . The dashed curves correspond to the case without bootstrap current and the solid curves to the case with current. (a) Enclosed toroidal bootstrap current. (b) Rotational transform profile. (c) Mercier stability criterion.

fluxes (a factor of 4/3 in favor of QSTK). We find that  $Q_i A$  is significantly reduced (by a factor 2-3) in QSTK compared to HSX for the range of gradients studied, demonstrating the success of the optimization strategy. The fluctuations in QSTK [fig. 3(d)] are relatively weak, and also less localized on the surface, compared to HSX [and most optimized stellarators, e.g. W7-X [5]], where the density fluctuations lie within a strip near the outboard midplane,  $\theta \sim 0$  [fig. 3(c)], owing to the more pronounced “bean-shaped” plane. Evaluation of the toroidal critical gradient (eq. 5) for HSX indicates a threshold of  $a/L_{T,crit} = 1.15$  on the outboard field line  $\alpha = 0$ , while a flux tube selected on the inboard ( $\alpha = \pi/4$ ) has the much larger predicted threshold of  $a/L_{T,crit} = 2.50$ . This suggests that the model (eq. 5) still captures the basic physics controlling the intensity of fluctuations on the surface in HSX, even far above the threshold.

*MHD stability and coils.*— QSTK, as a result of the  $f_{\text{well}}$  objective in the optimization [eq. 6)], also possesses a vacuum magnetic well and satisfies  $V'' < 0$  at all radial locations (not shown). An artificial, nearly linear (in  $r^2$ ) pressure profile  $T_i = T_e = 1 \text{ keV} * [1 - (r/a)^2]$ ,  $n_i = n_e = 4.4 * 10^{20} \text{ m}^{-3} * [1 - (r/a)^{10}]$ , corresponding to a volume-averaged  $\beta = 1.78\%$  (with volume-averaged  $B \simeq 1 \text{ T}$ ), is applied to the configuration. The resulting bootstrap current profile calculated with DKES [43–45]

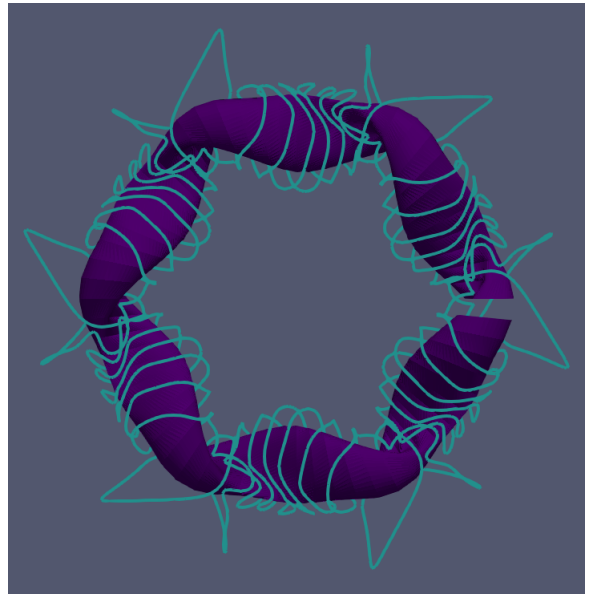


FIG. 5. Boundary surface of QSTK surrounded by electromagnetic coils

amounting to an integrated current of roughly 80 kA [fig. 4(a)]. Both the vacuum and bootstrap configurations produce rotational transform profiles that avoid crossing the resonance  $m/n = 6/4 = 3/2$  [Figs. 2(a), 4(b)]. The method of [46], which relies on the isomorphism between quasisymmetry and axisymmetry, was found to produce a similar bootstrap current profile for QSTK, although the results (not shown) were not in as good agreement as in cases with “precise” quasisymmetry [33]. Evaluations [47] of the Mercier criterion [48, 49] indicate that, for the configuration with pressure and bootstrap current included, the Mercier criterion is satisfied [fig. 4(b)] and the bootstrap current produces a stabilizing up-shift in  $D_M$  [50]. This result is in contrast to previous QH configurations with significant ITG turbulence reduction compared to HSX [18, 51], which, unlike HSX, violated Mercier stability. We also apply the coil optimization features of SIMSOPT to produce the magnetic field of QSTK, finding that the relative maximum field error can be reduced below 5% and a relative mean error below 1% with four unique coils (48 coils in total). The initial coil and MHD studies show that QSTK has potential for finite- $\beta$  (reactor-relevant) operation scenarios.

*Discussion and conclusions.*— We have not explored trapped electron mode stability [52, 53] as we expect flat density profiles in ECRH heated plasmas [1], especially at reactor scales. Electron temperature gradient (ETG) turbulence in QSTK is likely to benefit from the ITG optimization both linearly (from the isomorphism with ITG modes [14]) and nonlinearly (from the short connection length [54]) with regard to ETG losses. At high  $\beta$  values, turbulence is expected to transition from ITG to kinetic ballooning mode turbulence [25, 55]. This physics is delegated to a separate publication, in the framework of a

QSTK reactor study. More generally, the method developed here for calculating ITG critical gradients can also be applied to optimization of quasi-axisymmetric and quasi-isodynamic configurations. The design of turbulence optimized stellarators with improved ion confinement thus appears to now be within reach.

The authors thank P. Helander, A. Zocco, M. Landreman, and C. Beidler for helpful conversations. We thank J.F. Lobsien for help with initial coil optimization. This work was supported by a grant from the Simons Foundation (No. 560651, G. T. R.-C.). Computing resources

at the Cobra cluster at IPP Garching and the Marconi Cluster were used to perform the simulations. This work has been carried out within the framework of the EUROfusion Consortium, funded by the European Union via the Euratom Research and Training Programme (Grant Agreement No 101052200 — EUROfusion). Views and opinions expressed are however those of the author(s) only and do not necessarily reflect those of the European Union or the European Commission. Neither the European Union nor the European Commission can be held responsible for them.

- 
- [1] M. N.A. Beurskens, S. A. Bozhenkov, O. Ford, P. Xanthopoulos, A. Zocco, Y. Turkin, A. Alonso, C. Beidler, I. Calvo, D. Carralero, T. Estrada, G. Fuchert, O. Grulke, M. Hirsch, K. Ida, M. Jakubowski, C. Killer, M. Krychowiak, S. Kwak, S. Lazerson, A. Langenberg, R. Lunsford, N. Pablant, E. Pasch, A. Pavone, F. Reimold, Th Romba, A. Von Stechow, H. M. Smith, T. Windisch, M. Yoshinuma, D. Zhang, and R. C. Wolf, “Ion temperature clamping in Wendelstein 7-X electron cyclotron heated plasmas,” *Nuclear Fusion* **61**, 116072 (2021).
  - [2] J.-P. Bähner, J.A. Alcusón, S.K. Hansen, A. von Stechow, O. Grulke, T. Windisch, H.M. Smith, Z. Huang, E.M. Edlund, M. Porkolab, M.N.A. Beurskens, S.A. Bozhenkov, O.P. Ford, L. Vanó, A. Langenberg, N. Pablant, G.G. Plunk, A. Bañón Navarro, and F. Jenko, “Phase contrast imaging measurements and numerical simulations of turbulent density fluctuations in gas-fuelled ECRH discharges in Wendelstein 7-X,” *Journal of Plasma Physics* **87** (2021), 10.1017/s0022377821000635.
  - [3] D. Carralero, T. Estrada, E. Maragkoudakis, T. Windisch, J. A. Alonso, M. Beurskens, S. Bozhenkov, I. Calvo, H. Damm, O. Ford, G. Fuchert, J. M. García-Regaña, N. Pablant, E. Sánchez, E. Pasch, and J. L. Velasco, “An experimental characterization of core turbulence regimes in Wendelstein 7-X,” *Nuclear Fusion* **61** (2021), 10.1088/1741-4326/ac112f, arXiv:2105.05107.
  - [4] S. A. Bozhenkov, Y. Kazakov, O. P. Ford, M. N.A. Beurskens, J. Alcusón, J. A. Alonso, J. Baldzuhn, C. Brandt, K. J. Brunner, H. Damm, G. Fuchert, J. Geiger, O. Grulke, M. Hirsch, U. Höfel, Z. Huang, J. Knauer, M. Krychowiak, A. Langenberg, H. P. Laqua, S. Lazerson, N. B. Marushchenko, D. Moseev, M. Otte, N. Pablant, E. Pasch, A. Pavone, J. H.E. Proll, K. Rahbarnia, E. R. Scott, H. M. Smith, T. Stange, A. Von Stechow, H. Thomsen, Yu Turkin, G. Wurden, P. Xanthopoulos, D. Zhang, and R. C. Wolf, “High-performance plasmas after pellet injections in Wendelstein 7-X,” *Nuclear Fusion* **60**, 066011 (2020).
  - [5] P. Xanthopoulos, S. A. Bozhenkov, M. N. Beurskens, H. M. Smith, G. G. Plunk, P. Helander, C. D. Beidler, J. A. Alcusón, A. Alonso, A. Dinklage, O. Ford, G. Fuchert, J. Geiger, J. H.E. Proll, M. J. Pueschel, Y. Turkin, F. Warmer, and The W7 X. Team, “Turbulence Mechanisms of Enhanced Performance Stellarator Plasmas,” *Physical Review Letters* **125**, 75001 (2020).
  - [6] H. E. Mynick, N. Pomphrey, and P. Xanthopoulos, “Optimizing stellarators for turbulent transport,” *Physical Review Letters* **105**, 1–4 (2010).
  - [7] P. Xanthopoulos, H. E. Mynick, P. Helander, Y. Turkin, G. G. Plunk, F. Jenko, T. Görler, D. Told, T. Bird, and J. H.E. Proll, “Controlling turbulence in present and future stellarators,” *Physical Review Letters* **113**, 1–4 (2014).
  - [8] C. C. Hegna, P. W. Terry, and B. J. Faber, “Theory of ITG turbulent saturation in stellarators: Identifying mechanisms to reduce turbulent transport,” *Physics of Plasmas* **25** (2018), 10.1063/1.5018198.
  - [9] M. Nunami, T. H. Watanabe, and H. Sugama, “A reduced model for ion temperature gradient turbulent transport in helical plasmas,” *Physics of Plasmas* **20** (2013), 10.1063/1.4822337.
  - [10] C. C. Hegna, D. T. Anderson, A. Bader, T. A. Bechtel, A. Bhattacharjee, M. Cole, M. Drevlak, J. M. Duff, B. J. Faber, S. R. Hudson, M. Kotschenreuther, T. G. Kruger, M. Landreman, I. J. McKinney, E. Paul, M. J. Pueschel, J. S. Schmitt, P. W. Terry, A. S. Ware, M. Zarnstorff, and C. Zhu, “Improving the stellarator through advances in plasma theory,” *Nuclear Fusion* **62** (2022), 10.1088/1741-4326/ac29d0.
  - [11] G. T. Roberg-Clark, G. G. Plunk, and P. Xanthopoulos, “Calculating the linear critical gradient for the ion-temperature-gradient mode in magnetically confined plasmas,” *Journal of Plasma Physics* **87**, 905870306 (2021).
  - [12] G. T. Roberg-Clark, G. G. Plunk, and P. Xanthopoulos, “Coarse-grained gyrokinetics for the critical ion temperature gradient in stellarators,” *Physical Review Research* **4**, L032028 (2022).
  - [13] Alessandro Zocco, Linda Podavini, José Manuel García-Regaña, Michael Barnes, Felix I. Parra, A. Mishchenko, and Per Helander, “Gyrokinetic electrostatic turbulence close to marginality in the Wendelstein 7-X stellarator,” *Physical Review E* **106**, 1–6 (2022).
  - [14] F. Jenko, W. Dorland, and G. W. Hammett, “Critical gradient formula for toroidal electron temperature gradient modes,” *Physics of Plasmas* **8**, 4096–4104 (2001).
  - [15] H. Biglari, P. H. Diamond, and M. N. Rosenbluth, “Toroidal ion-pressure-gradient-driven drift instabilities and transport revisited,” *Physics of Fluids B* **1**, 109–118 (1989).
  - [16] J. A. Baumgaertel, G. W. Hammett, and D. R. Mikkelsen, “Comparing linear ion-temperature-gradient-

- driven mode stability of the National Compact Stellarator Experiment and a shaped tokamak,” Physics of Plasmas **20** (2013), 10.1063/1.4791657.
- [17] A. Zocco, P. Xanthopoulos, H. Doerk, J. W. Connor, and P. Helander, “Threshold for the destabilisation of the ion-temperature-gradient mode in magnetically confined toroidal plasmas,” Journal of Plasma Physics **84** (2018), 10.1017/S0022377817000988.
- [18] G. T. Roberg-Clark, P. Xanthopoulos, and G. G. Plunk, “Reduction of electrostatic turbulence in a quasi-helically symmetric stellarator via critical gradient optimization,” 1–15 (2022), arXiv:2210.16030.
- [19] G. G. Plunk, P. Helander, P. Xanthopoulos, and J. W. Connor, “Collisionless microinstabilities in stellarators. III. the ion-temperature-gradient mode,” Physics of Plasmas **21** (2014), 10.1063/1.4868412.
- [20] A. J. Brizard and T. S. Hahm, “Foundations of nonlinear gyrokinetic theory,” Reviews of Modern Physics **79**, 421–468 (2007).
- [21] R. L. Dewar and A. H. Glasser, “Ballooning mode spectrum in general toroidal systems,” Physics of Fluids **26**, 3038–3052 (1983).
- [22] J. W. Connor, R. J. Hastie, and J. B. Taylor, “Shear, periodicity, and plasma ballooning modes,” Physical Review Letters **40**, 396–399 (1978).
- [23] J.H.E. Proll, G.G. Plunk, B.J. Faber, T. Görler, P. Helander, I.J. McKinney, M.J. Pueschel, H.M. Smith, and P. Xanthopoulos, “Turbulence mitigation in maximum-J stellarators with electron-density gradient,” Journal of Plasma Physics **88** (2022), 10.1017/s002237782200006x.
- [24] R. Jorge and M. Landreman, “Ion-temperature-gradient stability near the magnetic axis of quasisymmetric stellarators,” Plasma Physics and Controlled Fusion **63** (2021), 10.1088/1361-6587/abfdd4, arXiv:2102.12390.
- [25] M. J. Pueschel, M. Kammerer, and F. Jenko, “Gyrokinetic turbulence simulations at high plasma beta,” Physics of Plasmas **15**, 102310 (2008).
- [26] F. Jenko and W. Dorland, “Prediction of Significant Tokamak Turbulence at Electron Gyroradius Scales,” Physical Review Lett **89**, 25001–1 (2002).
- [27] G. G. Plunk, P. Xanthopoulos, and P. Helander, “Distinct Turbulence Saturation Regimes in Stellarators,” Physical Review Letters **118**, 1–5 (2017), arXiv:1703.03257.
- [28] H. Sugama, “Damping of toroidal ion temperature gradient modes,” Physics of Plasmas **6**, 3527–3535 (1999).
- [29] F. Romanelli, “Ion temperature-gradient-driven modes and anomalous ion transport in tokamaks,” Physics of Fluids B **1**, 1018–1025 (1989).
- [30] Felix Warmer, K. Tanaka, P. Xanthopoulos, M. Nunami, M. Nakata, C. D. Beidler, S. A. Bozhenkov, M. N.A. Beurskens, K. J. Brunner, O. P. Ford, G. Fuchert, H. Funaba, J. Geiger, D. Gradic, K. Ida, H. Igami, S. Kubo, A. Langenberg, H. P. Laqua, S. Lazerson, T. Morisaki, M. Osakabe, N. Pablant, E. Pasch, B. Peterson, S. Satake, R. Seki, T. Shimozuma, H. M. Smith, T. Stange, A. V. Stechow, H. Sugama, Y. Suzuki, H. Takahashi, T. Tokuzawa, T. Tsujimura, Y. Turkin, R. C. Wolf, I. Yamada, R. Yanai, R. Yasuhara, M. Yokoyama, Y. Yoshimura, M. Yoshinuma, D. Zhang, and W7-X Team, “Impact of Magnetic Field Configuration on Heat Transport in Stellarators and Heliotrons,” Physical Review Letters **127**, 225001 (2021).
- [31] Matt Landreman, Bharat Medasani, Florian Wechsung, Andrew Giuliani, Rogerio Jorge, and Caoxiang Zhu, “SIMSOPT: A flexible framework for stellarator optimization,” Journal of Open Source Software **6**, 3525 (2021).
- [32] S. P. Hirshman and J. C. Whitson, “Steepest-descent moment method for three-dimensional magnetohydrodynamic equilibria,” Physics of Fluids **26**, 3553–3568 (1983).
- [33] Matt Landreman and Elizabeth Paul, “Magnetic Fields with Precise Quasisymmetry for Plasma Confinement,” Physical Review Letters **128**, 35001 (2022).
- [34] Sven Stroteich, Pavlos Xanthopoulos, Gabriel Plunk, and Ralf Schneider, “Seeking turbulence optimized configurations for the Wendelstein 7-X stellarator : ion temperature gradient and electron temperature gradient turbulence,” Journal of Plasma Physics **88**, 175880501 (2022).
- [35] V. V. Nemov, S. V. Kasilov, W. Kernbichler, and M. F. Heyn, “Evaluation of 1/v neoclassical transport in stellarators,” Physics of Plasmas **6**, 4622–4632 (1999).
- [36] T. K. Mau, T. B. Kaiser, A. A. Grossman, A. R. Raffray, X. R. Wang, J. F. Lyon, R. Maingi, L. P. Ku, and M. C. Zarnstorff, “Divertor configuration and heat load studies for the ARIES-CS fusion power plant,” Fusion Science and Technology **54**, 771–786 (2008).
- [37] Rogerio Jorge, “rogeriojorge/NEAT: First release of NEAT - NEar-Axis opTimisation code (v0.1), <https://doi.org/10.5281/zenodo.6622018>,” (2022).
- [38] Christopher G. Albert, Sergei V. Kasilov, and Winfried Kernbichler, “Symplectic integration with non-canonical quadrature for guiding-center orbits in magnetic confinement devices,” Journal of Computational Physics **403**, 109065 (2020), arXiv:1903.06885.
- [39] H. Maaßberg, C. D. Beidler, and E. E. Simmet, “Density control problems in large stellarators with neoclassical transport,” Plasma Physics and Controlled Fusion **41**, 1135–1153 (1999).
- [40] F. Jenko, W. Dorland, M. Kotschenreuther, and B. N. Rogers, “Electron temperature gradient driven turbulence,” Physics of Plasmas **7**, 1904–1910 (2000).
- [41] P. Xanthopoulos, G. G. Plunk, A. Zocco, and P. Helander, “Intrinsic turbulence stabilization in a stellarator,” Physical Review X **6**, 1–5 (2016).
- [42] J. N. Talmadge, F. S. B. Anderson, D. T. Anderson, C. Deng, W. Guttenfelder, K. M. Likin, J. Lore, J. C. Schmitt, and K. Zhai, “Experimental Tests of Quasisymmetry in HSX,” Plasma and Fusion Research **3**, S1002–S1002 (2008).
- [43] S. P. Hirshman, K. C. Shaing, W. I. van Rij, C. O. Beasley, and E. C. Crume, “Plasma transport coefficients for nonsymmetric toroidal confinement systems,” Physics of Fluids **29**, 2951–2959 (1986).
- [44] W. I. Van Rij and S. P. Hirshman, “Variational bounds for transport coefficients in three-dimensional toroidal plasmas,” Physics of Fluids B **1**, 563–569 (1989).
- [45] C. D. Beidler, H. M. Smith, A. Alonso, T. Andreeva, J. Baldzuhn, M. N.A. Beurskens, M. Borchardt, S. A. Bozhenkov, K. J. Brunner, H. Damm, M. Drevlak, O. P. Ford, G. Fuchert, J. Geiger, P. Helander, U. Hergenhahn, M. Hirsch, U. Höfel, Ye O. Kazakov, R. Kleiber, M. Krychowiak, S. Kwak, A. Langenberg, H. P. Laqua, U. Neuner, N. A. Pablant, E. Pasch, A. Pavone, T. S. Pedersen, K. Rahbarnia, J. Schilling, E. R. Scott, T. Stange, J. Svensson, H. Thomsen, Y. Turkin,

- F. Warmer, R. C. Wolf, D. Zhang, I. Abramovic, S. Äkäslompolo, J. Alcusón, P. Aleynikov, K. Aleynikova, A. Ali, A. Alonso, G. Anda, E. Ascasibar, J. P. Bähner, S. G. Baek, M. Balden, M. Banduch, T. Barbui, W. Behr, A. Benndorf, C. Biedermann, W. Biel, B. Blackwell, E. Blanco, M. Blatzheim, S. Ballinger, T. Bluhm, D. Böckenhoff, B. Böswirth, L. G. Böttger, V. Bor-suk, J. Boscary, H. S. Bosch, R. Brakel, H. Brand, C. Brandt, T. Bräuer, H. Braune, S. Brezinsek, K. J. Brunner, R. Burhenn, R. Bussiahn, B. Buttenschön, V. Bykov, J. Cai, I. Calvo, B. Cannas, A. Cappa, A. Carls, L. Carraro, B. Carvalho, F. Castejon, A. Charl, N. Chaudhary, D. Chauvin, F. Chernyshev, M. Cian-ciosa, R. Citarella, G. Claps, J. Coenen, M. Cole, M. J. Cole, F. Cordella, G. Cseh, A. Czarnecka, K. Czerski, M. Czerwinski, G. Czymek, A. da Molin, A. da Silva, A. de la Pena, S. Degenkolbe, C. P. Dhard, M. Di-bon, A. Dinklage, T. Dittmar, P. Drewelow, P. Drews, F. Durodie, E. Edlund, F. Effenberg, G. Ehrke, S. El-getti, M. Endler, D. Ennis, H. Esteban, T. Estrada, J. Fellinger, Y. Feng, E. Flom, H. Fernandes, W. H. Fi-etz, W. Figacz, J. Fontdecaba, T. Fornal, H. Frerichs, A. Freund, T. Funaba, A. Galkowski, G. Gantenbein, Y. Gao, J. García Regaña, D. Gates, B. Geiger, V. Gian-nella, A. Gogoleva, B. Goncalves, A. Goriaev, D. Gradic, M. Grahl, J. Green, H. Greuner, A. Grosman, H. Grote, M. Gruca, O. Grulke, C. Guerard, P. Hacker, X. Han, J. H. Harris, D. Hartmann, D. Hathiramani, B. Hein, B. Heinemann, P. Helander, S. Henneberg, M. Henkel, U. Hergenhahn, J. Hernandez Sanchez, C. Hidalgo, K. P. Hollfeld, A. Höltig, D. Höschen, M. Houry, J. Howard, X. Huang, Z. Huang, M. Hubeny, M. Huber, H. Hunger, K. Ida, T. Ilkei, S. Illy, B. Israeli, S. Jablon-ski, M. Jakubowski, J. Jelonnek, H. Jenzsch, T. Jesche, M. Jia, P. Junghanns, J. Kacmarczyk, J. P. Kallmeyer, U. Kamionka, H. Kasahara, W. Kasperek, N. Ken-mochi, C. Killer, A. Kirschner, T. Klinger, J. Knauer, M. Knaup, A. Knieps, T. Kobarg, G. Kocsis, F. Köchl, Y. Kolesnichenko, A. Könies, R. König, P. Kornejew, J. P. Koschinsky, F. Köster, M. Krämer, R. Krampitz, A. Krämer-Flecken, N. Krawczyk, T. Kremeyer, J. Krom, I. Ksiazek, M. Kubkowska, G. Kühner, T. Kurki-Suonio, P. A. Kurz, M. Landreman, P. Lang, R. Lang, S. Langish, H. Laqua, R. Laube, S. Lazerson, C. Lechte, M. Lennartz, W. Leonhardt, C. Li, C. Li, Y. Li, Y. Liang, C. Linsmeier, S. Liu, J. F. Lobsien, D. Loesser, J. Loizu Cisquella, J. Lore, A. Lorenz, M. Losert, A. Lücke, A. Lumsdaine, V. Lutsenko, H. Maaßberg, O. Marchuk, J. H. Matthew, S. Marsen, M. Marushchenko, S. Masuzaki, D. Maurer, M. Mayer, K. McCarthy, P. McNeely, A. Meier, D. Mellein, B. Mendelevitch, P. Mertens, D. Mikkelsen, A. Mishchenko, B. Missal, J. Mittelstaedt, T. Mizuchi, A. Mollen, V. Moncada, T. Mönnich, T. Morisaki, D. Moseev, S. Murakami, G. Náfrádi, M. Nagel, D. Nau-joks, H. Neilson, R. Neu, O. Neubauer, T. Ngo, D. Nicolai, S. K. Nielsen, H. Niemann, T. Nishizawa, R. Nocentini, C. Nührenberg, J. Nührenberg, S. Ober-mayer, G. Offermanns, K. Ogawa, J. Ölmanns, J. On-gena, J. W. Oosterbeek, G. Orozco, M. Otte, L. Pa-cios Rodriguez, N. Panadero, N. Panadero Alvarez, D. Papenfuß, S. Paqay, E. Pawelec, T. S. Pedersen, G. Pelka, V. Perseo, B. Peterson, D. Pilopp, S. Pin-gel, F. Pisano, B. Plaum, G. Plunk, P. Pölöskei, M. Porkolab, J. Proll, M. E. Puiatti, A. Puig Sitjes, F. Purps, M. Rack, S. Récsei, A. Reiman, F. Reimold, D. Reiter, F. Remppel, S. Renard, R. Riedl, J. Rie-mann, K. Risze, V. Rohde, H. Röhlinger, M. Romé, D. Rondeshagen, P. Rong, B. Roth, L. Rudischhauser, K. Rummel, T. Rummel, A. Runov, N. Rust, L. Ryc, S. Ryosuke, R. Sakamoto, M. Salewski, A. Samart-sev, M. Sanchez, F. Sano, S. Satake, J. Schacht, G. Satheeswaran, F. Schauer, T. Scherer, A. Schlaich, G. Schlisio, F. Schluck, K. H. Schlüter, J. Schmitt, H. Schmitz, O. Schmitz, S. Schmuck, M. Schneider, W. Schneider, P. Scholz, R. Schrittweis, M. Schröder, T. Schröder, R. Schroeder, H. Schumacher, B. Schweer, S. Sereda, B. Shanahan, M. Sibilia, P. Sinha, S. Sipilä, C. Slaby, M. Slezcka, W. Spiess, D. A. Spong, A. Spring, R. Stadler, M. Stejner, L. Stephey, U. Stridde, C. Suzuki, V. Szabó, T. Szabolics, T. Szepesi, Z. Szőkefalvi-Nagy, N. Tamura, A. Tancetti, J. Terry, J. Thomas, M. Thumm, J. M. Travere, P. Traverso, J. Treter, H. Trimino Mora, H. Tsuchiya, T. Tsujimura, S. Tulipán, B. Unterberg, I. Vakulchyk, S. Valet, L. Vanó, P. van Eeten, B. van Milligen, A. J. van Vuuren, L. Vela, J. L. Velasco, M. Vergote, M. Vervier, N. Vianello, H. Viebke, R. Vilbrandt, A. von Stechow, A. Vorköper, S. Wadle, F. Wagner, E. Wang, N. Wang, Z. Wang, T. Wauters, L. Wegener, J. Weggen, T. Wegner, Y. Wei, G. Weir, J. Wendorf, U. Wenzel, A. Werner, A. White, B. Wiegel, F. Wilde, T. Windisch, M. Winkler, A. Winter, V. Winters, S. Wolf, R. C. Wolf, A. Wright, G. Wurden, P. Xanthopoulos, H. Yamada, I. Yamada, R. Yasuhara, M. Yokoyama, M. Zanini, M. Zarnstorff, A. Zeitler, H. Zhang, J. Zhu, M. Zilker, A. Zocco, S. Zoltanik, and M. Zuin, “Demonstration of reduced neoclassical energy transport in Wendelstein 7-X,” *Nature* **596**, 221–226 (2021).
- [46] M. Landreman, S. Buller, and M. Drevlak, “Optimization of quasi-symmetric stellarators with self-consistent bootstrap current and energetic particle confinement,” *Physics of Plasmas* **29** (2022), 10.1063/5.0098166, arXiv:2205.02914.
- [47] J. „urgen N.“uhrenberg and Regine Zille, “Equilibrium and Stability of low-shear Stellarators,” in *Theory of Fusion Plasmas Varenna 1987* (Societ`a Italiana di Fisica, Bologna, 1987) p. 3.
- [48] C. Mercier, “Crit\`ere de stabilit\`e d’un syst\`eme toroi\`dal hydromagn\`etique en pression scalaire,” in *Plasma Physics and Controlled Nuclear Fusion Research 1961, 2* (International Atomic Energy Agency, Vienna, 1962) p. 801.
- [49] Matt Landreman and Rogerio Jorge, “Magnetic well and Mercier stability of stellarators near the magnetic axis,” *Journal of Plasma Physics* (2020), 10.1017/S002237782000121X, arXiv:2006.14881.
- [50] L. P. Ku and A. H. Boozer, “New classes of quasi-helically symmetric stellarators,” *Nuclear Fusion* **51** (2011), 10.1088/0029-5515/51/1/013004.
- [51] A. Bader, B. J. Faber, J. C. Schmitt, D. T. Anderson, M. Drevlak, J. M. Duff, H. Frerichs, C. C. Hegna, T. G. Kruger, M. Landreman, I. J. McKinney, L. Singh, J. M. Schroeder, P. W. Terry, and A. S. Ware, “Advancing the physics basis for quasi-helically symmetric stellarators,” *Journal of Plasma Physics* **1**, 1–24 (2020).
- [52] J. H.E. Proll, P. Helander, J. W. Connor, and G. G. Plunk, “Resilience of quasi-isodynamic stellarators against trapped-particle instabilities,” *Physical Review*

- Letters **108**, 7–10 (2012).
- [53] R. J.J. Mackenbach, J. H.E. Proll, and P. Helander, “Available Energy of Trapped Electrons and Its Relation to Turbulent Transport,” Physical Review Letters **128**, 175001 (2022), arXiv:2109.01042.
- [54] G. G. Plunk, P. Xanthopoulos, G. M. Weir, S. A. Bozhenkov, A. Dinklage, G. Fuchert, J. Geiger, M. Hirsch, U. Hoefel, M. Jakubowski, A. Langenberg, N. Pablant, E. Pasch, T. Stange, and D. Zhang, “Stellarators Resist Turbulent Transport on the Electron Larmor Scale,” Physical Review Letters **122**, 35002 (2019).
- [55] K. Aleynikova, A. Zocco, P. Xanthopoulos, P. Helander, and C. Nührenberg, “Kinetic ballooning modes in tokamaks and stellarators,” Journal of Plasma Physics **84**, 1–16 (2018).